





Distinct Roles of Glutamine Metabolism in Benign and Malignant Cartilage Tumors With *IDH* Mutations

Hongyuan Zhang,^{1,2}  Vijitha Puvindran,² Puvindran Nadesan,² Xiruo Ding,³  Leyao Shen,^{1,2,4} Yuning J Tang,⁵ Hidetoshi Tsushima,⁶ Yasuhito Yahara,^{7,8} Ga I Ban,² Guo-Fang Zhang,^{9,10} Courtney M Karner,^{1,2,4}  and Benjamin A. Alman^{1,2} 

¹Department of Cell Biology, Duke University, Durham, NC, USA

²Department of Orthopaedic Surgery, Duke University, Durham, NC, USA

³Department of Biomedical Informatics and Medical Education, University of Washington, Seattle, WA, USA

⁴Department of Internal Medicine, University of Texas Southwestern Medical Center, Dallas, TX, USA

⁵Department of Genetics, Stanford University, Stanford, CA, USA

⁶Department of Orthopaedic Surgery, Kyushu University, Fukuoka, Japan

⁷Department of Molecular and Medical Pharmacology, Faculty of Medicine, University of Toyama, Toyama, Japan

⁸Department of Orthopaedic Surgery, Faculty of Medicine, University of Toyama, Toyama, Japan

⁹Sarah W. Stedman Nutrition and Metabolism Center and Duke Molecular Physiology Institute, Duke University Medical Center, Durham, NC, USA

¹⁰Department of Medicine, Endocrinology and Metabolism Division, Duke University Medical Center, Durham, NC, USA

ABSTRACT

Enchondromas and chondrosarcomas are common cartilage neoplasms that are either benign or malignant, respectively. The majority of these tumors harbor mutations in either *IDH1* or *IDH2*. Glutamine metabolism has been implicated as a critical regulator of tumors with *IDH* mutations. Using genetic and pharmacological approaches, we demonstrated that glutaminase-mediated glutamine metabolism played distinct roles in enchondromas and chondrosarcomas with *IDH1* or *IDH2* mutations. Glutamine affected cell differentiation and viability in these tumors differently through different downstream metabolites. During murine enchondroma-like lesion development, glutamine-derived α -ketoglutarate promoted hypertrophic chondrocyte differentiation and regulated chondrocyte proliferation. Deletion of glutaminase in chondrocytes with *Idh1* mutation increased the number and size of enchondroma-like lesions. In contrast, pharmacological inhibition of glutaminase in chondrosarcoma xenografts reduced overall tumor burden partially because glutamine-derived non-essential amino acids played an important role in preventing cell apoptosis. This study demonstrates that glutamine metabolism plays different roles in tumor initiation and cancer maintenance. Supplementation of α -ketoglutarate and inhibiting GLS may provide a therapeutic approach to suppress enchondroma and chondrosarcoma tumor growth, respectively. © 2022 The Authors. *Journal of Bone and Mineral Research* published by Wiley Periodicals LLC on behalf of American Society for Bone and Mineral Research (ASBMR).

KEY WORDS: GLUTAMINE METABOLISM; CARTILAGE TUMORS; GROWTH PLATE; ISOCITRATE DEHYDROGENASE; CHONDROCYTE DIFFERENTIATION

Introduction

Enchondroma is a common benign cartilaginous neoplasm and is estimated to be present in 3% of the total population.^(1,2) These tumors develop from dysregulated chondrocyte differentiation in the growth plate and are mostly present in the metaphysis of long bones.⁽³⁾ In patients with multiple enchondromatosis (more than one enchondroma lesion) such as Maffucci's syndrome and Ollier's disease, the risk of malignant

transformation is reported to be up to 60%.⁽⁴⁾ Chondrosarcoma is the second most common primary malignancy of the bone.⁽⁴⁾ They arise de novo or develop from preexisting benign tumors including enchondromas.⁽⁴⁾ High-grade chondrosarcomas have high metastatic potential and poor prognosis.⁽⁵⁾ Currently there are no universally effective pharmacologic therapies for enchondromas or chondrosarcomas.

Somatic mutations of isocitrate dehydrogenase 1 and 2 (*IDH1* and *IDH2*) are the most frequent genetic variations in enchondromas and chondrosarcomas.⁽⁶⁻¹⁰⁾ They are present in 56% to

This is an open access article under the terms of the [Creative Commons Attribution-NonCommercial-NoDerivs](https://creativecommons.org/licenses/by-nc-nd/4.0/) License, which permits use and distribution in any medium, provided the original work is properly cited, the use is non-commercial and no modifications or adaptations are made.

Received in original form November 10, 2021; revised form February 2, 2022; accepted February 21, 2022.

Address correspondence to: Benjamin A. Alman, MD, 311 Trent Drive, Durham, NC 27705, USA. E-mail: ben.alman@duke.edu

Additional Supporting Information may be found in the online version of this article.

Journal of Bone and Mineral Research, Vol. 37, No. 5, May 2022, pp 983–996.

DOI: 10.1002/jbmr.4532

© 2022 The Authors. *Journal of Bone and Mineral Research* published by Wiley Periodicals LLC on behalf of American Society for Bone and Mineral Research (ASBMR).

90% of enchondroma tumors^(6,8) and in about 50% of chondrosarcoma tumors.^(7,9) Although *IDH1* and *IDH2* mutations are present in enchondromas and chondrosarcomas, it is not known whether these tumors share similar metabolic requirements for tumor development and cell viability. Wild-type *IDH1* and *IDH2* enzymes catalyze the reversible conversion between isocitrate and α -ketoglutarate (α -KG) in the cytoplasm or the mitochondria, respectively. Mutant *IDH1* and *IDH2* enzymes lose their original function and gain a neomorphic function that converts α -KG to D-2-hydroxyglutarate (D-2HG).⁽¹¹⁻¹³⁾ D-2HG is considered as a putative “oncometabolite” in various cancers with mutations in *IDH1/2*.⁽¹⁴⁻²⁰⁾ Interestingly, pharmacological inhibition of mutant *IDH1* enzyme did not alter chondrosarcoma tumorigenesis despite effective reduction of D-2HG synthesis.⁽²¹⁾ Several clinical trials of mutant *IDH* inhibitors have been conducted in patients with chondrosarcoma.⁽²²⁾ The results to date have been variable, showing at best stabilization of the disease.⁽²²⁾ Recently, an investigation of the metabolomes in chondrosarcomas showed global alterations in cellular metabolism in *IDH1* or *IDH2* mutant chondrosarcomas, suggesting such alteration might drive the neoplastic phenotype or be possible therapeutic targets for cancers with *IDH1* or *IDH2* mutations.⁽²³⁾

Glutamine metabolism is an important metabolic pathway that is critical for the survival of various cancers as well as proper proliferation and differentiation of different cell types.⁽²⁴⁻³⁰⁾ Glutamine metabolism starts when glutaminase (GLS) deaminates glutamine to glutamate. Glutamate could be further used to generate α -ketoglutarate (α -KG), glutathione, other non-essential amino acids, and nucleotides, etc. Through different downstream metabolites, glutamine regulates cancer cell behaviors by modulating bioenergetics, biosynthesis, redox homeostasis, etc.⁽²⁵⁾ In cancers with *IDH1* or *IDH2* mutations, glutamine is utilized as the primary source for D-2HG production.^(11,31,32) In addition, some tumors with *IDH1* or *IDH2* mutations are reported to be dependent on glutamine metabolism for tumor growth or cell viability.⁽³³⁻³⁶⁾ In non-cancerous cells, glutamine metabolism regulates cell differentiation mainly through downstream metabolites, including amino acids, α -KG, and acetyl-CoA.^(27,29,37,38)

In the context of cartilage tumors, it is unknown how glutamine regulates tumor development in enchondroma and cancer cell survival in chondrosarcoma. We therefore used a genetically engineered mouse model of enchondroma and primary human chondrosarcoma samples to address these questions. Here we identified that GLS was upregulated in both human patient chondrosarcoma samples with mutations in *IDH1* or *IDH2* and murine chondrocytes with *Idh1* mutation. However, deleting *Gls* in the mouse led to increased number and size of benign tumor-like lesions and affected hypertrophic chondrocyte differentiation, likely due to a reduction of α -KG; whereas inhibiting GLS in *IDH1* or *IDH2* mutant chondrosarcomas led to a smaller tumor size and a reduction in cell viability, associated with the compromised production of non-essential amino acids. Collectively, these data highlight a previously unknown stage-dependent role of glutamine metabolism in cartilage tumors and may provide a therapeutic approach for the malignant cartilage tumor chondrosarcoma.

Materials and Methods

Animals

Idh1^{LSL/+}, *Gls*^{fl/fl} (JAX: #017894), *Col2a1Cre*, *Col2a1Cre*^{ERT2}, and NOD *scid* gamma (NSG) mice are as previously described.^(26,39-43)

43) Congenic animals were used in every experiment. *Idh1*^{LSL/+} mice bear a conditional knock-in of the point mutation *IDH1*-R132Q as previously clarified.⁽³⁹⁾ Mice were housed on a 12-hour light and dark cycle with free access to water and Pico-Lab Rodent Diet 20 (LabDiet #5053, St. Louis, MO, USA) at 23°C. All animal procedures were approved by the institutional animal care and use committee at Duke University.

Isolation of primary chondrocytes

Primary sternal chondrocyte isolation was as described before.⁽⁴⁴⁾ In brief, mouse sterna and ribs from P3 neonates were cleaned and digested by pronase (Roche, Indianapolis, IN, USA; 11459643001) at 2 mg/mL PBS at 37°C with constant agitation for 1 hour, Collagenase IV (Worthington, Lakewood, NJ, USA; LS004189) at 3 mg/mL DMEM at 37°C for 1 hour, Collagenase IV at 0.5 mg/mL DMEM at 37°C for 3 hours, and filtered using 45 μ m cell strainer.

Cell culture

Chondrocytes were cultured in high-glucose DMEM with 10% FBS and 1% penicillin/streptomycin. High-glucose DMEM was used to maintain the growth and identity of primary costal chondrocytes. Primary chondrosarcoma cells were cultured in α -MEM with 10% FBS and 1% penicillin/streptomycin. In some experiments, chondrocytes and chondrosarcoma cells were treated with 10 μ M Bis-2-(5-phenylacetamido-1,2,4-thiadiazol-2-yl)ethyl sulfide (BPTES), 100 μ M epigallocatechin gallate (EGCG), 500 μ M aminooxyacetate (AOA), 2X non-essential amino acids, or DMSO as indicated for indicated 48 hours. Cells were cultured at 37°C in a humidified 5% CO₂ incubator.

Transfection

In indicated experiment, chondrocytes were transfected with adenovirus-GFP and adenovirus-Cre at 400 MOI.

RNA isolation and qPCR

Total RNA isolation was isolated using Trizol and chloroform. An amount of 1 mL Trizol was added to cell pellet. After resuspension, the tubes were incubated at room temperature for 10 minutes. Then 200 μ L of chloroform was added to the tube and mixed well. After centrifugation at maximum speed for 10 minutes, the solution was separated into three layers. The top layer of aqueous phase solution was transferred to a clean tube and mixed with 200 μ L of isopropanol to precipitate RNA. After incubation at room temperature for 10 minutes, the tube was centrifuged at maximum speed for 10 minutes, and supernatant was discarded. RNA pellet was washed with 70% ethanol two times. After that, RNA was dissolved in molecular-grade water.

An amount of 1 μ g RNA was used to synthesize cDNA through reverse transcription using iScript cDNA synthesis kit. Quantitative real-time PCR (qPCR) was then performed using the Powerup SYBR green reagent (Invitrogen, Carlsbad, CA, USA; A25777) on a QuantStudio 3 real-time PCR system (Thermo Fisher Scientific, Waltham, MA, USA). Relative gene expression was calculated and normalized to a housekeeping gene (beta-actin) using the 2^{- $\Delta\Delta$ Ct} method.

Western blotting

Cultured chondrocytes were lysed in RIPA buffer containing protease and phosphatase inhibitor tablet (Roche, 11836170001, and Sigma [St. Louis, MO, USA], 4906845001, respectively). Protein concentration was quantified using the BCA method (Pierce, Rockford, IL, USA). Proteins were resolved on 8% polyacrylamide gels and transferred onto Immuno-Blot PVDF membrane (Bio-Rad, Hercules, CA, USA). After the wet transfer, the membranes were blocked for 1 hour at room temperature in 5% milk powder in TBS with 0.1% Tween (TBST) and then incubated at 4°C with the primary antibody (Anti-Glutaminase antibody: Abcam [Cambridge, MA, USA] AB93434; Anti- β -actin: Invitrogen MA5-15739) overnight. Membranes were washed three times with TBST and further incubated with anti-rabbit IgG, HRP-linked antibody (RRID: AB_2099233) in 5% milk (in TBST) for 1 hour at room temperature. All blots were developed using either enhanced or normal chemiluminescence (Clarity Substrate Kit, Bio-Rad).

Metatarsal organ culture

The second, third, and fourth metatarsal bones were dissected from the hindlimbs of embryos at E16.5. They were transferred to 24-well non-adherent plates with 1 mL α -MEM supplemented with 50 μ g/mL ascorbic acid, 1 mM β -glycerophosphate, and 0.2% bovine serum albumin. The media was changed every other day. Explants were cultured at 37°C in a humidified 5% CO₂ incubator for 5 days and then fixed with 10% neutral buffered formalin (NBF).

EdU assay

EdU assay (Thermo Fisher Scientific, C10337) was performed according to the manufacturer's instructions. In brief, cells were cultured with 10 mM EdU for 12 hours before fixation with 4% PFA/PBS for 15 minutes and permeabilization with 0.5% Triton X-100 for 20 minutes at room temperature. Cells were then incubated with Click-iT reaction cocktail for 30 minutes in the dark at room temperature and stained with DAPI.

TUNEL assay

TUNEL assay was performed according to the manufacturer's instructions (Roche, 11684795910). In brief, cells were fixed with 4% PFA/PBS at room temperature for 1 hour and permeabilized with 0.1% Triton X-100 in 0.1% sodium citrate for 2 minutes on ice. After rinse with PBS, cells were incubated with TUNEL reaction mixture at 37°C for 1 hour and stained with DAPI.

Cell viability assay

Cell viability was determined by CellTiter-Glo Assay according to the manufacturer's instructions (Promega, Madison, WI; G7570). In brief, CellTiter-Glo Buffer was thawed at room temperature and transferred to CellTiter-Glo Substrate. Cell culture plate was equilibrated to room temperature for 30 minutes. An amount of 100 μ L CellTiter-Glo Reagent was added to the cell culture media in each well. The plate was mixed for 2 minutes on an orbital shaker and incubated for 10 minutes at room temperature. Luminescence was then recorded. Cell viability of each primary chondrosarcoma patient sample was normalized to the average cell viability in the vehicle group of the same sample.

Annexin V/PI staining

Annexin V and Propidium Iodide staining was performed according to the manufacturer's instructions (Invitrogen R37176 and P1304MP). In brief, 1 drop of Annexin V APC Ready Flow Conjugate was added to 0.5 mL of annexin-binding buffer with 2.5 mM calcium. Then 1 mg/mL PI was added to the APC binding buffer with 1/1000 dilution. The cells were incubated for 15 minutes at room temperature. Fluorescence was detected by flow cytometry.

GLS activity assay

Primary chondrocytes were cultured before the experiment. After washing cells with Hanks' Buffered Saline Solution (HBSS) three times, cells were cultured in α -MEM-containing media containing 2 μ M Glutamine and 4 mCi/mL L-[3,4-³H(N)]-Glutamine (PerkinElmer, Waltham, MA, USA; NET551250UC). GLS activity was terminated by washing cells with ice-cold HBSS three times followed by scraping cells with 1 mL ice-cold milliQ water. Cells were lysed by sonication for 1 minute with 1-second pulse at 20% amplitude. Cell lysates were bound onto AG 1-X8 polyprep anion exchange column. Uncharged glutamine was eluted with 2 mL of milliQ water three times. Negatively charged glutamate and downstream metabolites were eluted with 2 mL of 0.1 M HCl three times. After adding 4 mL of scintillation cocktail to the eluent, DPM of the solution was measured by a Beckman Coulter (Brea, CA, USA) LS6500 Scintillation counter.

Xenograft

Before the experiment, chondrosarcoma cells from each patient's tumor were maintained subcutaneously *in vivo* in NSG mice. For the xenograft experiment, tumors were surgically removed from each mouse and divided into explants of 5 \times 5 \times 5 mm each, and implanted into the subcutaneous tissue on the back of NSG mice. BPTES and vehicle control (10% DMSO/PBS) treatment started 10 days after implantation. Mice were treated with BPTES at 0.2 g/kg or vehicle via intraperitoneal injection daily for 14 days. Tumor weights were recorded upon harvest. For each patient-derived xenograft experiment, relative tumor weight was determined by normalizing the tumor weight of each tumor to the average tumor weight of the vehicle control group.

Histological analysis

Bone histomorphometry for adult mice was performed on hindlimbs fixed in 10% neutral buffered formalin for 3 days followed by decalcification with 14% EDTA for 2 weeks at room temperature. Histomorphometry for embryonic skeletons was performed on tibias fixed in 10% neutral buffered formalin overnight followed by decalcification with 14% EDTA overnight at room temperature. After decalcification, skeletons were embedded in paraffin and sectioned at 5 μ m thickness. Safranin O staining was performed following standard protocol. Animals of both sexes were used for analysis. Hindlimbs from the left side were used for histological analyses. For quantification, each data point represents one individual animal.

Immunohistochemistry

Immunohistochemistry was performed on 5- μ m paraffin-sectioned limbs. For type X collagen, antigen retrieval was

performed by citrate buffer incubation at 85°C for 15 minutes and hyaluronidase digestion at 10 mg/mL at 37°C for 30 minutes. For BrdU staining, BrdU labeling reagent (Invitrogen, 000103) was injected into pregnant female mice at 1 mL/100 g body weight 2 hours before euthanasia. Antigen retrieval was performed by proteinase K digestion at 10 µg/mL at room temperature for 10 minutes. For MMP13, antigen retrieval was performed by hyaluronidase digestion at 5 mg/mL at 37°C for 30 minutes. For all immunohistochemistry, endogenous peroxidase activity was blocked by incubation with 3% H₂O₂/Methanol for 10 minutes followed by incubation with Dako Dual Endogenous Enzyme Block reagent (Agilent Dako, Santa Clara, CA; S2003) for 30 minutes at room temperature. The specimen was blocked with 2% horse serum at room temperature for 30 minutes followed by incubation with antibodies for Col X (1:500, Thermo Fisher Scientific, 14-9771-82), BrdU (1:1000, Thermo Fisher Scientific, MA3-071), MMP13 (1:100, MilliporeSigma, Burlington, MA, USA; MAB13424) overnight at 4°C. TUNEL assay was performed according to the manufacturer's instructions (Roche, 11684795910). In brief, the tissue was incubated with proteinase K at 10 µg/mL at room temperature for 20 minutes and then in TUNEL labeling reagent 37°C for 1 hour. Animals with both sexes were used for analysis. Hindlimbs from the left side were used for histological analyses. For quantification, each data point represents one individual animal. Quantification of the length of hypertrophic zone and bone elements was done using the image processing software Fiji Image J.

In situ hybridization

In situ hybridization was performed on 5-µm paraffin-sectioned limbs. Paraffin sections were deparaffinized and rehydrated, followed by fixation with 4% PFA at room temperature for 15 minutes. Sections were then treated with 20 µg/mL proteinase K for 15 minutes at room temperature, fixed with 4% PFA at room temperature for 10 minutes, and acetylation solution [1.33% triethanolamine, 0.175% HCl (37%), 0.375% acetic anhydride in MilliQ water] for 10 minutes. Sections were then incubated with hybridization buffer at 58°C for 3 hours, and then incubated with Digoxigenin-labeled RNA probe (*Col2a1*, *Pth1r*, *Col10a1*) at 58°C overnight. Sections were then washed with 5x SSC for one time at 65°C, followed by RNase A treatment at 37°C for 30 minutes. Sections were then washed 2x SSC for one time, 0.2x SSC for two times at 65°C, and then blocked with 2% Boehringer Blocking Reagent/20% Heat Inactivated Sheep Serum for 1 hour. Sections were then blocked with Anti-Digoxigenin antibody (1:4000 in blocking solution) at 4°C overnight. Sections were developed with BM Purple at room temperature until color developed. Animals of both sexes were used for analysis. Hindlimbs from the left side were used for histological analyses. For quantification, each data point represents one individual animal.

Analysis of enchondroma-like lesions and trabecular bone volume

Tamoxifen was administered daily for 10 days at 100 mg/kg body weight/day via intraperitoneal injection starting at 4 weeks of age. Mice were euthanized at 6 months of age. Hindlimbs were harvested for analyzing growth-plate and enchondroma-like phenotype. Hip-joint cartilage was used for confirming DNA recombination. Quantification of enchondroma-like lesions was performed as previously described.⁽⁴⁴⁾ In brief, enchondroma-like lesions were first identified by Safranin O staining, which was

performed on one slide (2 sections, 5 µm/section) in every 10 consecutive slides (10 µm). We then examined every slide consecutively under the light microscope to identify lesions that did not span to the Safranin O-stained slide. The number of lesions were then recorded. For every Safranin O-stained slide, we manually outlined each lesion and measured the area of each lesion using the image processing software Fiji Image J. We estimated the lesion size of each animal by adding up the areas of all the lesions in that animal. The lesion size for each animal was normalized to the average lesion size of *Col2Cre^{ERT2};ldh1^{LSL/+}* animals. Quantification of trabecular bone volume was performed by adding up the trabecular bone surface of each Safranin O-stained slide. For every Safranin O-stained slide, we manually outlined the trabecular bone 1200 µm below the growth plates of each tibia and femur and measured the area of trabecular bones using the image processing software Fiji Image J. We estimated the lesion size of each animal by adding up the areas of all the trabecular bones in our region of interest in that animal. Animals of both sexes were used for analysis. Hindlimbs from the left side were used for histological analyses. For quantification, each data point represents one individual animal.

D-2HG measurement

D-2HG is analyzed by liquid chromatography–tandem mass spectrometry (LC/MS/MS). Cell culture media was collected from each sample. After adding 2-HG-²H₄ (internal standard), the sample was dried under nitrogen and derivatized by (+)-O,O'-diacetyl-L-tartaric anhydride (DATAN) for measurement.

Carbon isotope labeling

Chondrocytes were cultured in DMEM with 4500 mg/L Glucose and 4 mM ¹⁵C₅-Glutamine in 6-cm cell culture plates for specified times. Primary chondrosarcoma cells were cultured in α-MEM with 1000 mg/L Glucose and 2 mM ¹⁵C₅-Glutamine in 6-cm cell culture plates for specified times. Methanol (500 µL) was used to extract metabolites from each plate. After centrifugation at 13,800 g for 15 minutes, supernatant was dried at 37°C. The dried residues were resuspended in 25 µL of methoxylamine hydrochloride (2% [w/v] in pyridine) and incubated at 40°C for 1.5 hours in a heating block. After brief centrifugation, 35 µL of MTBSTFA + 1% TBDMS was added, and the samples were incubated at 60°C for 30 minutes. The derivatized samples were centrifuged for 5 minutes at 20,000g, and the supernatants were transferred to GC vials for GC–MS analysis. A modified GC–MS method was employed.⁽²²⁾ The injection volume was 1 µL, and samples were injected in splitless mode. GC oven temperature was held at 80°C for 2 minutes, increased to 280°C at 7°C/minute, and held at 280°C for a total run time of 40 minutes. GC–MS analysis was performed on an Agilent 7890B GC system equipped with a HP-5MS capillary column (30 m, 0.25 mm i.d., 0.25 µm-phase thickness; Agilent J&W Scientific, Santa Clara, CA, USA), connected to an Agilent 5977A Mass Spectrometer operating under ionization by electron impact (EI) at 70 eV. Helium flow was maintained at 1 mL/min. The source temperature was maintained at 230°C, the MS quad temperature at 150°C, the interface temperature at 280°C, and the inlet temperature at 250°C. Mass spectra were recorded in mass scan mode with m/z from 50 to 700.

¹³C-based stable isotope analysis

M₀, M₁, ..., M_n refers to the isotopologues containing n heavy atoms in a molecule. The stable isotope distribution of individual metabolites was measured by GC–MS as described above. The

isotopologue enrichment or labeling in this work refers to the corrected isotope distribution.^(23,24)

Gene expression of *GLS* from chondrosarcoma patient samples

We used retrospective data from RESOS INCA network of bone, collected from 102 cartilage tumors in different French hospitals. Multiple samples may be taken from each tumor and sequenced. More details about the experiment, such as RNA isolation method and profiling, can be found the original article.⁽⁴⁵⁾ For our purposes, we utilized IDH mutation information to categorize samples into two groups: *IDH1* or *IDH2* mutation ($n = 46$) and *IDH1* and *IDH2* wild type ($n = 98$). We examined several gene expression levels across these two groups and reported adjusted p value for *GLS* result (with Benjamini–Hochberg correction). All the data processing and calculation were performed using Bioconductor docker (devel), with R version 4.0.3 and Bioconductor version 3.13.

Quantification and statistical analysis

Statistical analyses were performed using GraphPad (La Jolla, CA, USA) Prism 9 software. Data were presented as mean \pm SEM, mean \pm SD, or mean \pm 95% as specified in each figure. Statistical significance was determined by two-tailed Student's t test

or one-way or two-way ANOVA with multiple comparisons test as specified in each figure.

Results

IDH1 or *IDH2* mutant chondrosarcomas cells exhibited increased glutamine contribution to anaplerosis and non-essential amino acids production

From a published data set showing mRNA profiling (E-MTAB-7264) of chondrosarcoma tumors,⁽⁴⁵⁾ we observed that expression of *GLS* was upregulated in chondrosarcomas with *IDH1* or *IDH2* mutations (Supplemental Fig. S1), indicating glutamine metabolism might be important for cartilage tumor with *IDH1* or *IDH2* mutation. To understand how glutamine was utilized in chondrosarcoma cells, we performed a carbon tracing experiment with $^{13}\text{C}_5$ -glutamine in chondrosarcoma cells derived from 3 patients, each with wild-type *IDH1* and *IDH2*, mutant *IDH1*, and mutant *IDH2*. ^{13}C contribution to downstream metabolites was determined by measuring the isotope-labeling pattern. To be utilized by a cell, glutamine is first deaminated to glutamate through *GLS*. After that, glutamate can be converted to α -KG, a key metabolite in the tricarboxylic acid (TCA) cycle (Fig. 1A). There was a significant amount of glutamate labeled with ^{13}C in chondrosarcomas of different genotypes (Fig. 1B). Importantly, the labeling of ^{13}C in glutamate was significantly higher in *IDH1* or *IDH2* mutant chondrosarcomas when compared with

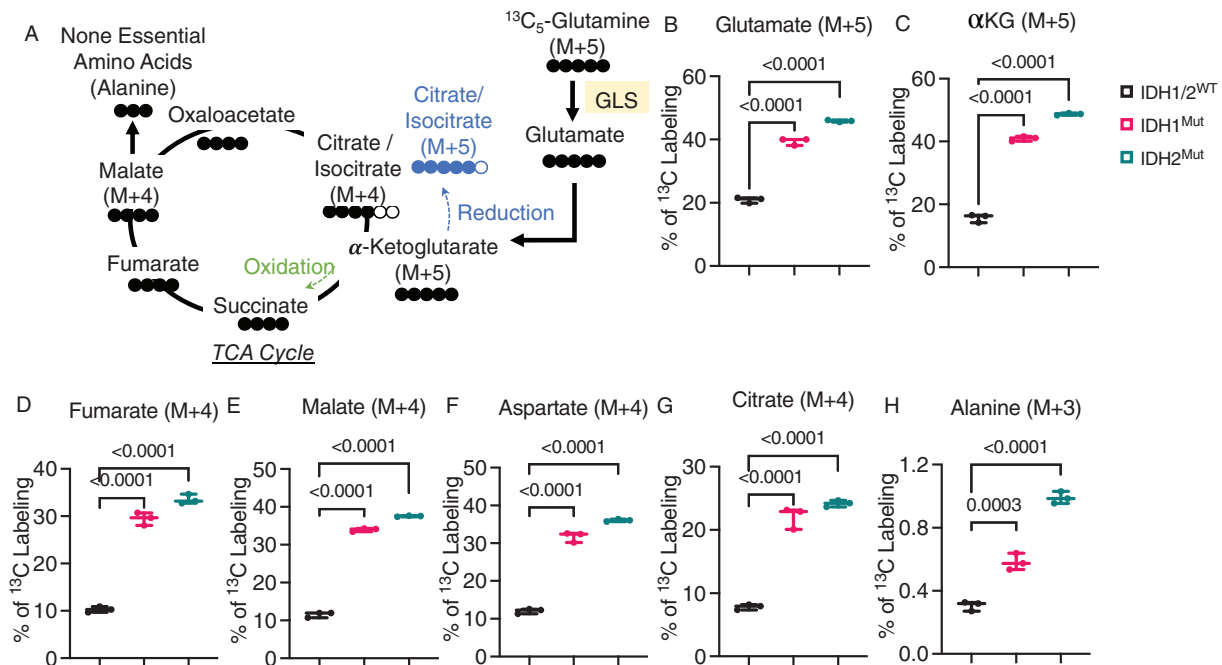


Fig. 1. Chondrosarcomas with *IDH1* or *IDH2* mutations had significantly increased contribution from glutamine carbon to downstream metabolites. (A) Graphical depiction of tracing glutamine metabolism using $^{13}\text{C}_5$ -glutamine. Filled circles indicate ^{13}C and open circles indicate ^{12}C . Green dashed line with arrowhead indicates the direction of oxidative decarboxylation. Blue dashed line with arrowhead indicates the direction of reductive carboxylation. (B–H) Percentage of $^{13}\text{C}_5$ -glutamine contribution to glutamate (B), α -ketoglutarate (C), fumarate (D), malate (E), oxaloacetate/aspartate (F), citrate (G), and alanine (H). The data represent three primary human chondrosarcoma samples each with wild-type *IDH1/2*, *IDH1* mutation, or *IDH2* mutation. Each data point represents technical replicates. Data are presented as box plots with indication of median; whiskers represent min to max values. The p values on the graph were determined by one-way ANOVA, Dunnett's multiple comparison tests. Results for ANOVA: (B) $F = 722.7$, $p < 0.0001$; (C) $F = 1099$, $p < 0.0001$; (D) $F = 433.6$, $p < 0.0001$; (E) $F = 2535$, $p < 0.0001$; (F) $F = 647.5$, $p < 0.0001$; (G) $F = 213.4$, $p < 0.001$; (H) $F = 208.0$, $p < 0.0001$.

chondrosarcoma cells with wild-type *IDH1* and *IDH2* (Fig. 1B). The ^{13}C labeling pattern was examined in the TCA cycle intermediates and non-essential amino acids. Chondrosarcomas with *IDH1* or *IDH2* mutations had significantly higher carbon contribution to all TCA cycle intermediates (Fig. 1C–G) and some non-essential amino acids such as alanine (Fig. 1H). Thus, *IDH1* or *IDH2* mutant chondrosarcomas were more efficient than *IDH1* and *IDH2* wild-type chondrosarcomas in converting glutamine to its downstream metabolites.

GLS was upregulated in IDH mutant chondrocytes

To understand the role of GLS in murine chondrocytes with *Idh1* mutation, we first examined whether expression of mutant *Idh1* gene could lead to altered GLS function. Expression of a mutant *IDH1*^{R132Q} enzyme in chondrocytes was shown to be sufficient to initiate enchondroma-like lesion formation in mice.⁽³⁹⁾ Chondrocytes were isolated from mice expressing the conditional *IDH1*^{R132Q} knock-in allele and transduced with adenovirus GFP or adenovirus Cre.⁽⁴⁶⁾ GLS activity in these chondrocytes was determined by measuring the conversion from radioactive ^3H -glutamine to radioactive ^3H -glutamate. In primary chondrocytes expressing mutant *IDH1*^{R132Q}, GLS activity was significantly upregulated by 2.5-fold (Fig. 2A).

To investigate how chondrocytes with wild-type and mutant *IDH1* enzymes utilize glutamine, we conducted ^{13}C tracing studies. In chondrocytes expressing the mutant *Idh1*, the percentage of ^{13}C labeling in glutamate (Fig. 2B), α -KG (Fig. 2C), other TCA cycle intermediates (Fig. 2D–G), and the non-essential amino acid alanine (Fig. 2H) was significantly increased.

Glutamine is a primary source for the production of D-2HG in *IDH1* or *IDH2* mutant cancers including chondrosarcoma.^(11,31,32) To examine whether glutamine is also the primary source for D-

2HG production in the murine chondrocytes expressing mutant *Idh1*, we cultured these chondrocytes with $^{13}\text{C}_5$ -glutamine and examined the percentage of ^{13}C -labeled D-2HG at different time points. After 10 hours, more than 80% of the D-2HG was labeled with ^{13}C , confirming glutamine is the primary source for D-2HG in *IDH1*^{R132Q} cells (Supplemental Fig. S2B). D-2HG was not detected in chondrocytes without *Idh1* mutation (Supplemental Fig. S2C). Thus, chondrocytes with an *Idh1* mutation showed increased GLS activity and more efficient conversion of glutamine to downstream metabolites.

GLS was important for chondrocyte differentiation and proliferation in chondrocytes with *Idh1* mutation

There are two isoforms of GLS, kidney-type GLS (encoded by *Gls*) and liver-type GLS (encoded by *Gls2*). Expression of *Gls2* was significantly lower than *Gls* in primary chondrocytes of both *Col2a1Cre*; *Idh1*^{LSL/+} and *Col2a1Cre* animals (Fig. 3A, GSE123130), consistent with the notion that GLS activity in chondrocytes was mainly catalyzed by *Gls*. We thus focused on *Gls* in the murine chondrocytes. To examine the role of *Gls* in vivo, we conditionally deleted *Gls* in these cells by crossing mice carrying a conditional null allele of *Gls* (*Gls*^{fl}) to the *Col2a1Cre* deleter mouse, which expresses Cre-recombinase in chondrocytes (Fig. 3B, C).^(40,41) *Col2a1Cre*; *Gls*^{fl/fl} chondrocytes had reduced glutamine uptake and glutamate production (Fig. 3D), confirming the function of GLS was efficiently deleted in these mice.

We first examined the phenotype of tibias in mice lacking *Gls* in chondrocytes using H&E staining (Fig. 3E). At embryonic (E) day 14.5, deleting *Gls* in *Idh1* wild-type chondrocytes or expressing mutant *Idh1* gene in chondrocytes did not cause a significant change in bone length (Fig. 4A). Deleting *Gls* in *Idh1* mutant chondrocytes significantly reduced the bone length (Fig. 4A). At E16.5

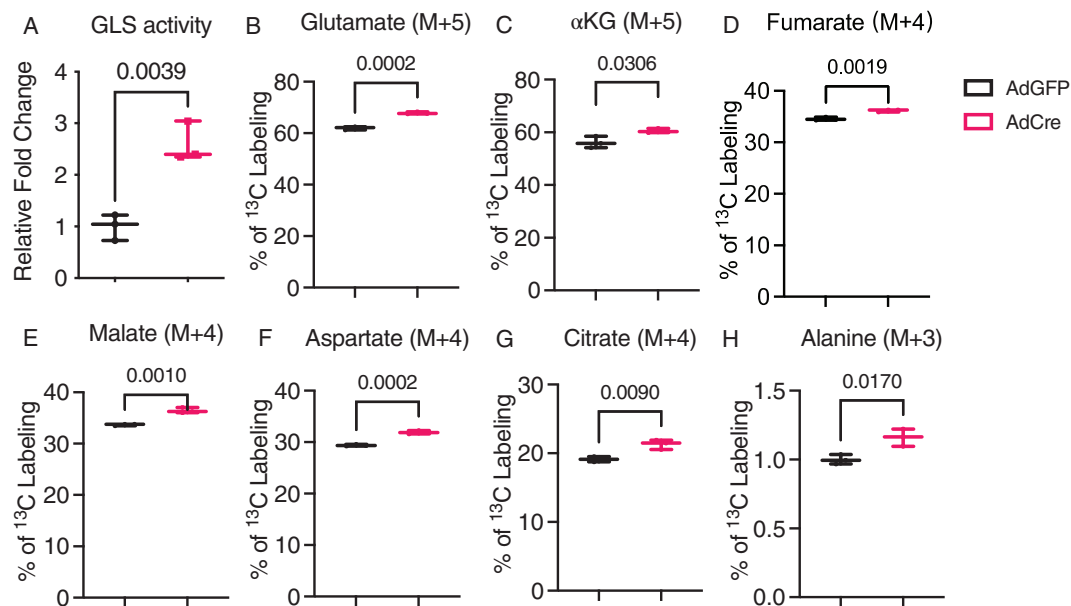


Fig. 2. Chondrocytes with *Idh1* mutation had increased GLS activity and glutamine contribution to downstream metabolites. (A) GLS activity of AdGFP; *Idh1*^{LSL/+} and AdCre;*Idh1*^{LSL/+} chondrocytes. (B–H) Percentage of $^{13}\text{C}_5$ -glutamine contribution to glutamate (B), α -ketoglutarate (C), fumarate (D), malate (E), oxaloacetate/aspartate (F), citrate (G), and alanine (H). Each data point represents individually transfected cell populations. Data are presented as box plots with indication of median; whiskers represent min to max values. The *p* values were determined by unpaired Student's *t* test.

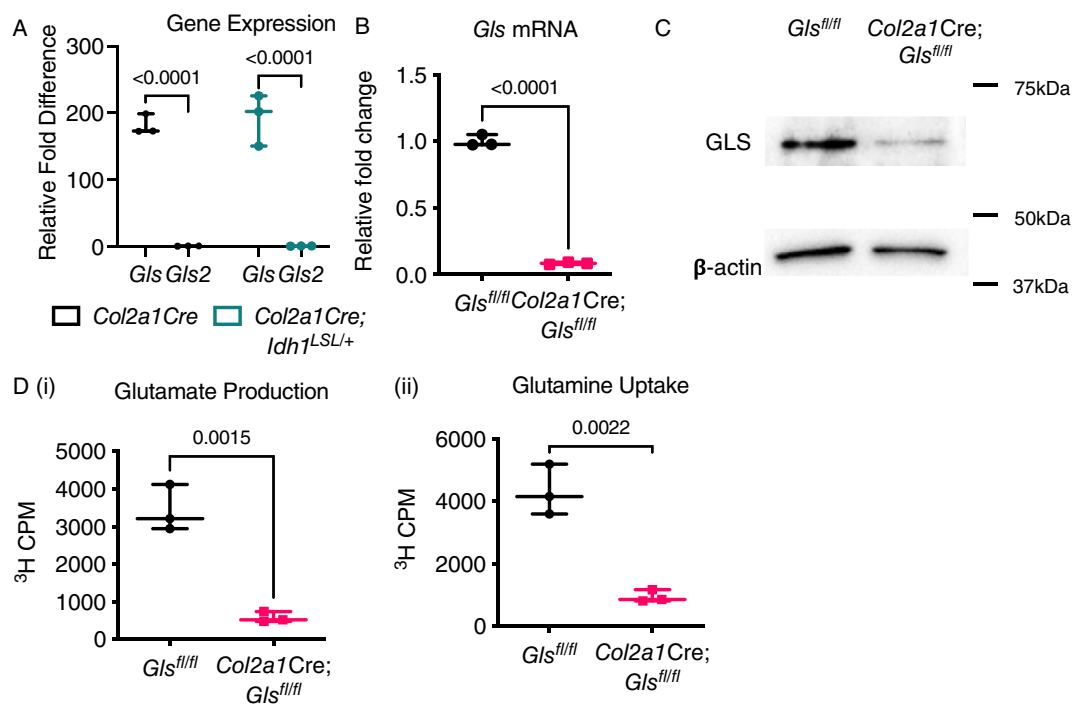


Fig. 3. *Gls* is the primary glutaminase isoform in chondrocytes. (A) Expression of *Gls* and *Gls2* in chondrocytes of *Col2a1Cre* and *Col2a1Cre;ldh1^{LSL/+}* animals. (B) Expression of *Gls* in chondrocytes of *Gls^{fl/fl}* and *Col2a1Cre;Gls^{fl/fl}* animals. (C) Western blot of GLS and β -Actin in chondrocytes of *Gls^{fl/fl}* and *Col2a1Cre;Gls^{fl/fl}* animals. (D) ³H-glutamate production (i) and ³H-glutamine uptake (ii) in chondrocytes of *Gls^{fl/fl}* and *Col2a1Cre;Gls^{fl/fl}* animals. For A, *p* values on the graph were determined by two-way ANOVA, Šidák's multiple comparisons test. $F(1, 8) = 243.7, p < 0.001$. For B and D, *p* values were determined by unpaired Student's *t* test.

and E18.5, we observed reduced bone length and defects in chondrocyte hypertrophic differentiation in *ldh1* mutant mice (Supplemental Fig. S3A–F), consistent with our previous report.⁽³⁹⁾ Deleting *Gls* did not cause an obvious skeletal phenotype in *ldh1* wild-type and *ldh1* mutant mice (Supplemental Fig. S3A–F).

We then used in situ hybridization to examine markers important for chondrocyte differentiation. Early chondrocyte marker *Col2a1* and pre-hypertrophic chondrocyte marker *Pth1r* were expressed by tibial chondrocytes at E14.5 (Fig. 4B, C). However, the regions between *Col2a1*-expressing cells and *Pth1r*-expressing cells were reduced in *ldh1* mutant animals. In *Gls;ldh1* double mutant mice, *Col2a1*-expressing cells and *Pth1r*-expressing cells became single regions in the middle of the bone with no separation (Fig. 4B, C). *Col10a1* is expressed by hypertrophic chondrocytes. At E14.5, the expression pattern of *Col10a1* was comparable among control, *Gls* mutant, and *ldh1* mutant mice, but in *Gls;ldh1* double mutant mice, there was reduced zone of staining (Fig. 4D, E). We also examined proliferation and apoptosis in these animals. No difference in proliferation was observed between control and *Gls* mutant animals in *ldh1* wild-type background, but proliferation was increased when *Gls* was deleted in *ldh1* mutant mice (Fig. 4F). Apoptosis was not detected in all animals at this stage based on immunohistochemistry of cleaved caspase 3 (Supplemental Fig. S3G).

Deleting GLS in chondrocytes increased the number and size of enchondroma-like lesions

We next examined how deleting *Gls* in chondrocyte postnatally affected chondrocyte homeostasis in growth plates and

enchondroma-like lesion formation in adult animals. We induced deletion of *Gls* at 4 weeks of age by tamoxifen and examined the phenotype at 6 months of age, a time point when growth plates were completely remodeled in control animals and enchondroma-like lesions were stable in *ldh1* mutant mice. Enchondroma-like lesions were identified in *ldh1* mutant animals as we previously reported and these animals showed less trabecular bone volume (Fig. 5A–D). No obvious growth plate phenotype was observed in *Gls* mutant mice, and histologic examination showed less trabecular bone (Fig. 5A, B). In contrast, the number and size of enchondroma-like lesions were significantly increased when *Gls* was deleted in *ldh1* mutant animals, and the trabecular bone volume was further reduced (Fig. 5A–D).

GLS regulated chondrocyte differentiation through α -ketoglutarate

Glutamine metabolism regulates chondrocyte differentiation through its downstream metabolites α -KG in *ldh1* wild-type background.⁽²⁷⁾ We examined whether GLS could regulate the differentiation of chondrocytes containing a *ldh1* mutation through α -KG. Our previous ¹³C tracing experiments showed α -KG was mainly derived from glutamine, and *ldh1* mutant chondrocytes were more efficient in converting glutamine to α -KG (Fig. 2C). We found the level of α -KG was reduced by more than 70% in *ldh1* mutant chondrocytes (Fig. 6A). Because chondrocytes with *ldh1* mutation were more efficient in converting glutamine to α -KG, the lower intracellular concentration was likely because α -KG was converted to D-2HG. When GLS was inhibited in *ldh1* mutant chondrocytes by Bis-2-(5-phenylacetamido-

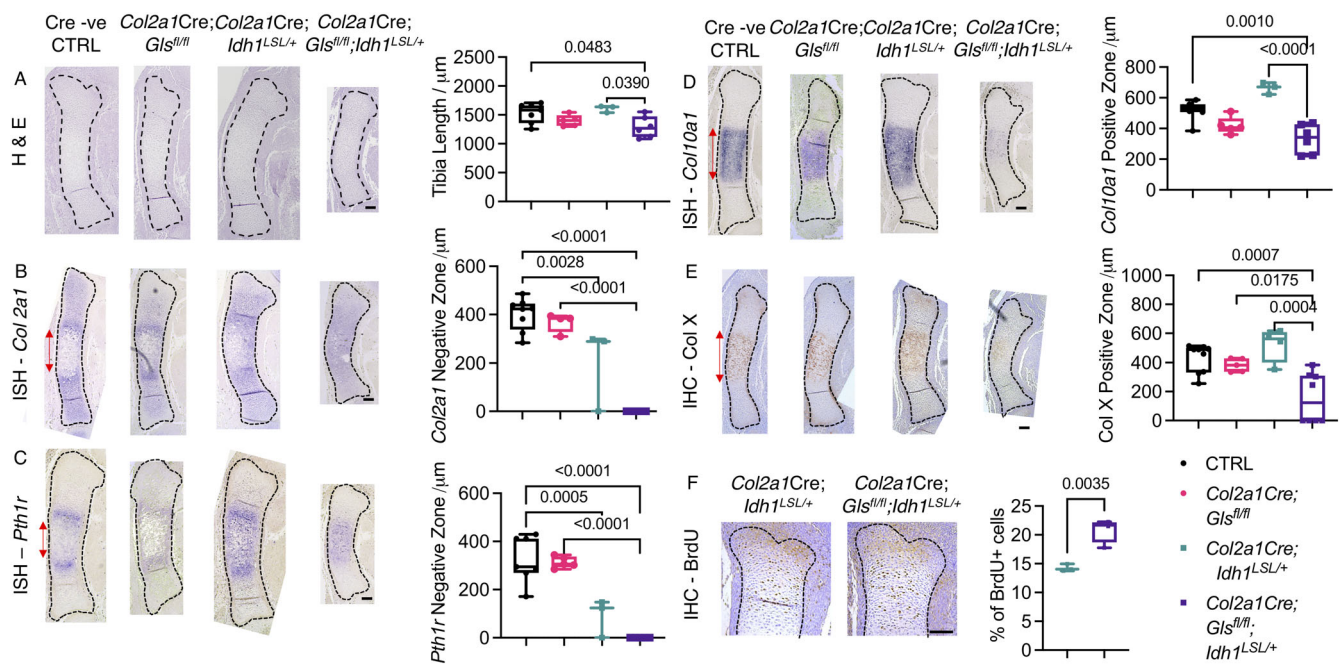


Fig. 4. Deleting GLS in *Col2a1Cre;ldh1^{LSL/+}* chondrocytes affected chondrocyte differentiation. (A) H&E staining and quantification of the length of tibias. (B) In situ hybridization of *Col2a1* and quantification of the length of *Col2a1*-negative zone. (C) In situ hybridization of *Pth1r* and quantification of the length of *Pth1r*-negative zone. (D) In situ hybridization of *Col10a1* and quantification of the length of *Col10a1*-positive zone. (E) Immunohistochemistry of Col X and quantification of the length of Col X-positive area. (F) Immunohistochemistry of BrdU and quantification of percentage of BrdU-positive cells. Each data point represents an individual animal. For A–E, *p* values were determined by one-way ANOVA, Tukey's multiple comparisons test. Results for ANOVA: (A) $F = 4.149$, $p = 0.0223$; (B) $F = 43.37$, $p < 0.0001$; (C) $F = 31.03$, $p < 0.001$; (D) $F = 16.92$, $p < 0.0001$; (E) $F = 10.83$, $p = 0.0001$. For F, the *p* value was determined by unpaired Student's *t* test. Data are presented as box plots with indication of median; whiskers represent min to max values. Scale bar = 100 μ m.

1,3,4-thiadiazol-2-yl)ethyl sulfide (BPTES), a small molecular inhibitor for GLS,⁽⁴⁷⁾ α -KG level was further reduced by about 60% (Fig. 6B).

Next, we investigated whether exogenous α -KG could rescue the defects of chondrocyte differentiation in *Col2a1Cre;Gls^{fl/fl};ldh1^{LSL/+}* animals. We injected cell-permeable dimethyl- α -KG (DM- α -KG) to pregnant dams every day from E11.5 to E13.5 and harvested the embryos at E14.5. Treatment with DM- α -KG rescued chondrocyte hypertrophy as *Col10a1* mRNA and COLX protein expression were both observed in *Gls;ldh1* double mutant mice (Fig. 6C–E). Finally, DM- α -KG treatment led to a modest decrease in proliferation (Fig. 6F, G) without inducing apoptosis (Fig. 6H).

Inhibiting GLS in *IDH1* or *IDH2* mutant chondrosarcoma xenografts reduced tumor weight

Previously it was reported that inhibiting GLS reduced viability in chondrosarcoma cell lines.⁽³⁵⁾ However, our murine data in enchondroma-like lesions suggests that GLS inhibition would have an opposite effect. We thus established patient-derived xenograft models as previously described to examine the effects of GLS inhibition in chondrosarcoma.⁽⁵¹⁾ We established and maintained chondrosarcoma xenografts by injecting primary patient chondrosarcoma cells into immune-deficient Nod-scid-gamma mice. We used five patient samples with *IDH1* mutation and one patient sample with wild-type *IDH1* and *IDH2*. All of these chondrosarcomas were histological grade 2/3. Chondrosarcoma tumors were divided into pieces

at 5 mm \times 5 mm \times 5 mm and implanted to immune-deficient Nod-scid-gamma mice subcutaneously. We treated these animals with BPTES or vehicle control for 14 days and measured the tumor weight at the time of death. No adverse effects were observed in these animals after BPTES or vehicle treatment. For each patient sample, the tumor weight of each mouse was normalized to the average tumor weight in the vehicle control group of the same patient sample. BPTES treatment significantly reduced tumor weight of chondrosarcoma tumors with *IDH1* mutations (Fig. 7B). We examined proliferation and apoptosis in each of these tumors using immunohistochemistry of Ki67 and cleaved caspase 3, respectively. BPTES treatment significantly increased apoptosis in chondrosarcoma xenografts, but we did not observe a substantial difference in proliferation (Fig. 7D). We then examined chondrosarcoma cells treated with BPTES in vitro. Consistent with our findings in vivo, BPTES treatment reduced cell viability, increased cell apoptosis, and did not alter proliferation in *IDH1* or *IDH2* mutant chondrosarcomas (Fig. 7E–G). Interestingly, BPTES treatment did not alter tumor burden of *IDH1* and *IDH2* wild-type chondrosarcoma (Supplemental Fig. S4). These data support previously published studies and show a different role of GLS in human chondrosarcoma than in murine enchondroma-like lesions.

Inhibition of GLS reduced the production of non-essential amino acids in chondrosarcoma

We next sought to understand how glutamine metabolism regulated cell survival of *IDH1* or *IDH2* mutant chondrosarcomas.

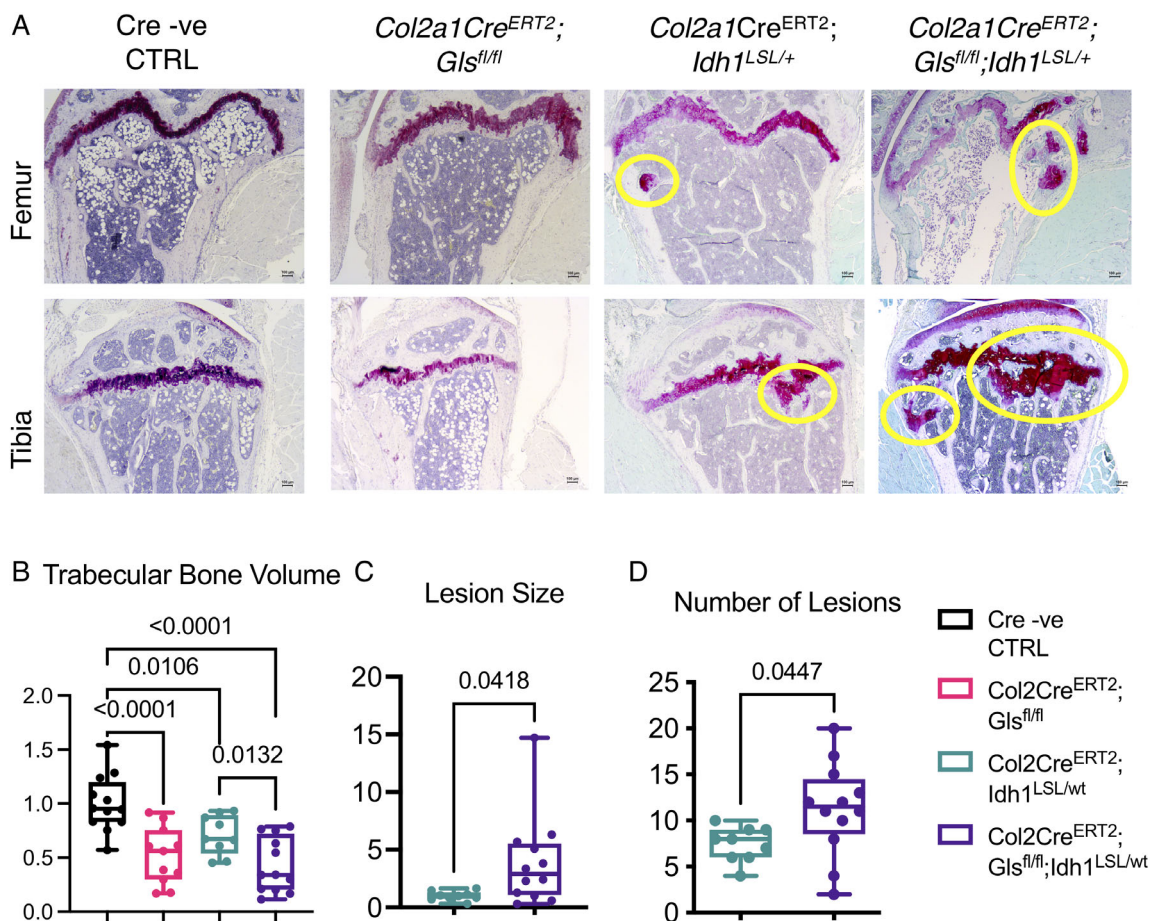


Fig. 5. Deleting *Gls* in *Col2a1Cre^{ERT2};ldh1^{LSL/+}* chondrocytes increased the number and size of enchondroma-like lesions. (A) Representative Safranin O staining of mice of specified genotypes. Enchondroma-like lesions are highlighted in yellow circles. (B) Quantification of the volume of trabecular bone based on Safranin O staining. (C, D) Quantification of the number (B) and size (C) of enchondroma-like lesions in animals of specified genotypes. Each data point represents an individual animal. Data are presented as box plots with indication of median; whiskers represent min to max values. For B, *p* values shown on the graph were determined by one-way ANOVA, Tukey's multiple comparisons test. $F = 12.57$, $p < 0.001$. For C and D, the *p* value was determined by unpaired Student's *t* test. Scale bar = 100 μ m.

Similar to in the mouse, α -KG levels were lower with BPTES treatment (Fig. 8A). However, unlike our murine findings, adding DM- α -KG did not rescue the apoptosis changes found with BEPTS treatment (Fig. 8B).

Downstream of GLS, glutamate could be further metabolized to α -KG through glutamate dehydrogenase and transaminases. Inhibiting transaminases by aminooxyacetate (AOA) caused a reduction of cell viability in *IDH1* or *IDH2* mutant chondrosarcomas similar to the effects of BPTES, but inhibiting glutamate dehydrogenase by epigallocatechin gallate (EGCG) did not affect cell survival (Fig. 8C). These data suggested transaminases might be more critical for chondrosarcoma cell survival downstream of GLS.

Non-essential amino acids can be produced from glutamine through GLS and then transaminases. They are known to play a role in regulating cancer apoptosis, raising the possibility that they may be playing this role in chondrosarcoma. We found lower levels of multiple non-essential amino acids when GLS was inhibited by BPTES (Fig. 8D). We treated these chondrosarcoma cells with non-essential amino acids, and in contrast to

our data from DM- α -KG, we found a modest rescue of apoptosis changes (Fig. 8E). However, supplementing non-essential amino acids to *Col2a1Cre;Gls^{fl/fl};ldh1^{LSL/+}* metatarsal organ culture did not lead to rescue of chondrocyte differentiation defects (Supplemental Fig. S5), suggesting they might not be the key mediator of the murine enchondroma-like lesions.

Discussion

In this study, we found that glutamine metabolism plays distinct roles in the tumor initiation of enchondroma and cancer maintenance of chondrosarcoma. Glutamine contribution to downstream metabolites was upregulated in chondrosarcomas and chondrocytes with mutations in *IDH1* or *IDH2* enzymes. During development of enchondroma, deleting *Gls* in murine chondrocytes with *ldh1* mutation interrupted hypertrophic differentiation during embryonic development and led to increased number and size of enchondroma-like lesions in adult animals. In malignant *IDH1* or *IDH2* mutant chondrosarcomas isolated

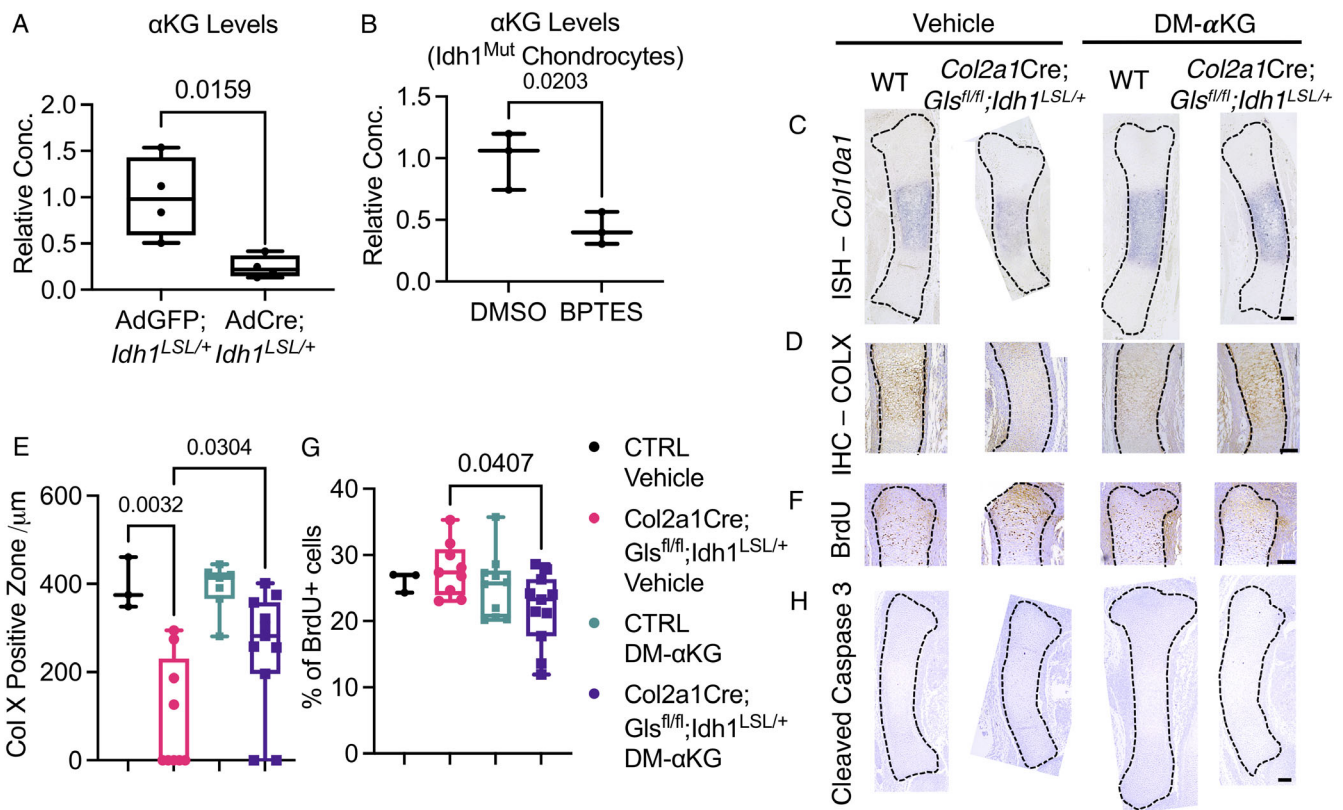


Fig. 6. GLS regulated *Col2a1Cre;ldh1^{LSL/+}* chondrocyte differentiation through the downstream metabolite α -KG. (A) Relative intracellular α -KG concentration in AdGFP;*ldh1^{LSL/+}* and AdCre;*ldh1^{LSL/+}* chondrocytes. (B) Relative intracellular α -KG concentration in AdCre;*ldh1^{LSL/+}* chondrocytes treated with vehicle control or 10 μ M BPTES. (C) In situ hybridization of *Col10a1*. (D) Immunohistochemistry of Col X. (E) Quantification of the length of Col X-positive zone. (F) Immunohistochemistry of BrdU. (G) Quantification of the percentage of BrdU-positive cells. (H) Immunohistochemistry of cleaved caspase 3. For A and B, each data point represents individually transfected cell populations. The *p* values were determined by unpaired Student's *t* test. For E and G, each data point represents an individual animal. The *p* values were determined by one-way ANOVA, Tukey's multiple comparisons test. Results for ANOVA: (E) $F = 10.54$, $p = 0.0001$; (F) $F = 2.774$, $p = 0.0592$. Data are presented as box plots with indication of median; whiskers represent min to max values. Scale bar = 100 μ m.

from human patients, pharmacological inhibition of GLS led to reduced tumor weight.

The distinct roles of glutamine metabolism in enchondroma and chondrosarcoma were possibly due to different metabolic needs at different stages of tumor development. We observed that supplementation of α -KG and non-essential amino acids rescued the defects in chondrocyte differentiation and chondrosarcoma apoptosis, respectively. As enchondroma rises from dysregulated chondrocyte differentiation, α -KG—the regulator for cell differentiation—plays an important role in the development of the benign tumor. For malignant chondrosarcomas, changes in differentiation might not be critical for tumor growth. However, these *IDH1* or *IDH2* mutant cancer cells might require some amino acids to support cell viability.

Molecular mechanisms underlying the distinct roles of glutamine metabolism in cartilage tumors remain to be further investigated. α -KG is reported to regulate cell fate mainly through epigenetic regulation by serving as a co-factor for 2-oxoglutarate-dependent oxygenases as well as precursor for other downstream metabolites. In mouse embryonic stem cells, α -KG suppressed cell differentiation by promoting demethylation of DNA, demethylation of repressive histone marks, and

demethylation of active histone mark through TET-family of DNA demethylase and Jumonji C-domain containing histone demethylases.^(49,50) In the context of chondrocyte differentiation, Stegen and colleagues reported *Gls* regulated chondrocyte differentiation through α -KG and its downstream metabolite acetyl-CoA postnatally via regulating histone acetylation.⁽²⁷⁾ Because enchondroma develops from dysregulated chondrocyte differentiation, it is possible that α -KG could affect expression of chondrogenic genes through altering histone modifications and DNA methylation. In malignant cancers, glutamine supported cancer cell proliferation and suppressed apoptosis and autophagy through producing other non-essential amino acids.⁽⁵¹⁻⁵⁵⁾ Non-essential amino acids mixture provides seven non-essential amino acids: alanine, asparagine, aspartate, glycine, serine, proline, and glutamate. Many of them have been shown to be critical for cancer cell viability, especially under metabolic stress. In glioblastoma and neuroblastoma, glutamine deprivation induced apoptosis, which could be restored by exogenous asparagine.⁽⁵⁵⁾ In pancreatic cancer, aspartate becomes “essential” when glutamine availability or metabolism is limited.⁽⁵⁶⁾ Glutamine could also regulate cancer cell viability through sustaining cellular redox homeostasis.⁽²⁵⁾ For the next

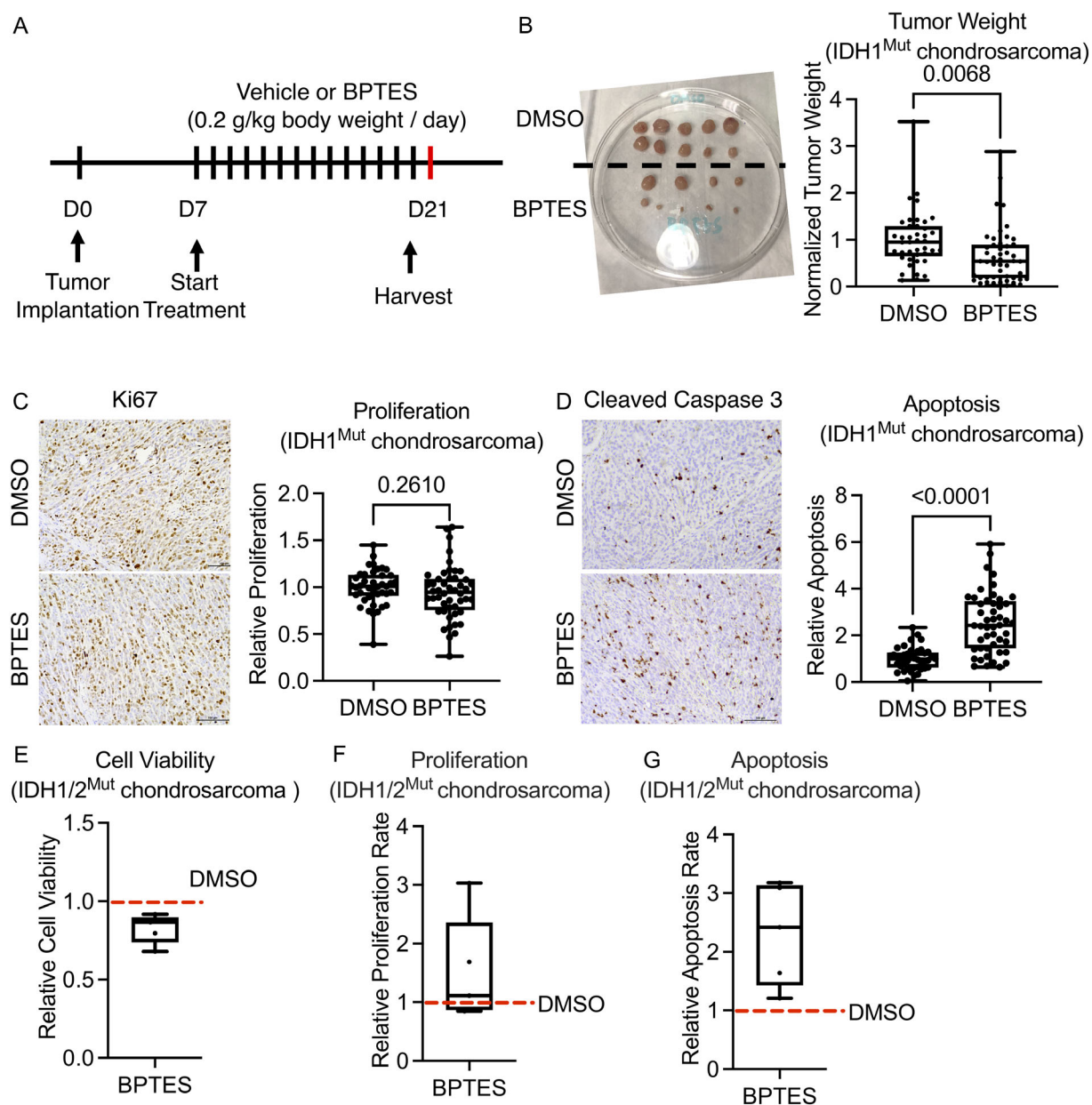


Fig. 7. Inhibiting GLS reduced tumor weight and induced apoptosis in chondrosarcomas with *IDH* mutations. (A) Experimental design for the xenograft experiment. (B) Representative pictures of xenografted tumor at the time of harvest and relative tumor weight of xenografted chondrosarcoma tumors at the time of harvest. (C) Representative picture of immunohistochemistry of Ki67 of xenografted tumors and quantification of relative proliferation of each tumor determined by percentage of Ki67-positive cells. (D) Representative picture of immunohistochemistry of cleaved caspase 3 of xenografted tumors and relative apoptotic of each tumor determined by percentage of cleaved caspase 3-positive cells. (E) Relative cell viability of *IDH1/2*^{Mut} chondrosarcoma cells treated with 10 μ M BPTES determined by CellTiter Glo cell viability assay. (F) Relative proliferation rate of *IDH1* or *IDH2* mutant chondrosarcoma cells treated with 10 μ M BPTES in vitro determined by EdU staining. (G) Relative apoptosis of *IDH1* or *IDH2* mutant chondrosarcoma cells treated with 10 μ M BPTES in vitro determined by TUNEL staining. For B–D, each data point represents one tumor. The *p* value was determined by unpaired Student's *t* test. For E–G, each data point represents the average of three technical triplicates of one patient sample. Data are presented as box plots with indication of median; whiskers represent min to max values.

step, it will be important to understand which and how non-essential amino acid(s) prevent apoptosis in *IDH1* or *IDH2* mutant chondrosarcomas.

One limitation of this study is that we studied the role of glutamine metabolism in enchondromas and chondrosarcomas using mouse models and human patient samples, respectively.

Thus, it is possible the distinct roles of glutamine metabolism we observed were caused by different metabolic needs of murine and human cells. To address this concern, it will be important to establish mouse models to study chondrosarcoma and to determine the role of glutamine metabolism in human enchondroma samples.

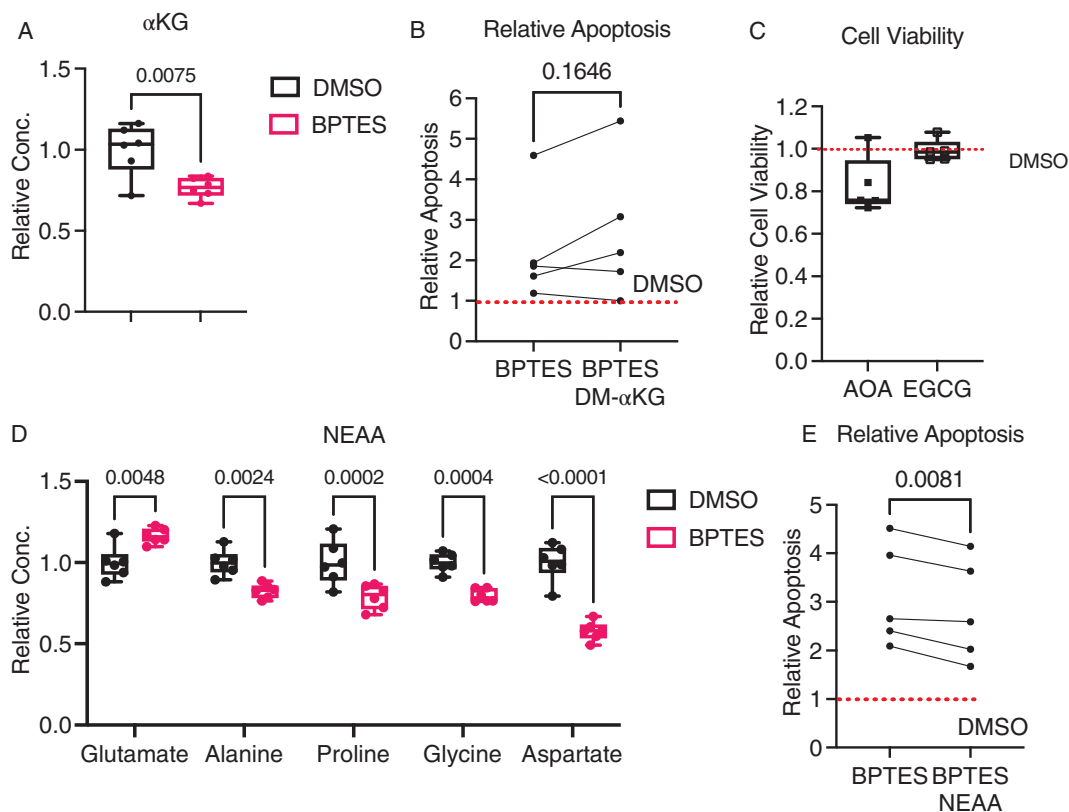


Fig. 8. GLS regulated cell apoptosis of chondrosarcomas with *IDH1* or *IDH2* mutations through production of non-essential amino acids. (A) Relative concentration of α -KG in *IDH1* or *IDH2* mutant chondrosarcomas treated with 10 μ M BPTES. (B) Relative apoptosis of *IDH1* or *IDH2* mutant chondrosarcoma cells treated with 10 μ M BPTES, or 10 μ M BPTES + 1 mM DM- α -ketoglutarate determined by Annexin V staining. (C) Relative cell viability of *IDH1/2*^{Mut} chondrosarcoma cells treated with 100 μ M AOA and 500 μ M EGCG. Each dot represents one patient sample. (D) Relative concentration of different amino acids in *IDH1* or *IDH2* mutant chondrosarcomas treated with 10 μ M BPTES. (E) Relative apoptosis of *IDH1* or *IDH2* mutant chondrosarcoma cells treated 10 μ M BPTES, or 10 μ M BPTES + 2X NEAA determined by Annexin V staining. For B, C, and E, each dot represents one patient sample. For A, unpaired Student's *t* test was used to determine *p* value. For B and E, paired Student's *t* test was used to determine *p* values. For D, *p* values are determined by two-way ANOVA, Šidák's multiple comparisons test. $F(1, 50) = 65.22, p < 0.0001$. Data are presented as box plots with indication of median; whiskers represent min to max values.

In summary, our study showed that GLS-mediated glutamine metabolism played distinct roles in *IDH1* or *IDH2* mutant enchondromas and chondrosarcomas through different downstream metabolites. In the context of enchondroma, deleting GLS in chondrocytes with *Idh1* mutation reduced the intracellular levels of α -KG, thus impairing hypertrophic differentiation and increasing cell proliferation and leading to increased number and size of enchondroma-like lesions. In chondrosarcoma, GLS regulated cell apoptosis partially by producing non-essential amino acids. This study demonstrates that glutamine metabolism plays different roles in the tumor initiation and cancer maintenance in cartilage tumors. Supplementation of α -ketoglutarate and inhibiting GLS may provide a therapeutic approach to suppress enchondroma and chondrosarcoma tumor growth, respectively.

Disclosures

HZ is a current employee of Amgen Inc. All other authors state that they have no conflicts of interest.

Acknowledgments

Research reported in this publication was supported by the National Institute of Arthritis and Musculoskeletal and Skin Diseases of the National Institutes of Health under award R01AR066765. The content is solely the responsibility of the authors and does not necessarily represent the official views of the National Institutes of Health.

Authors' roles: HZ: conceptualization, data curation, formal analysis, investigation, methodology, project administration, resources, validation, visualization, writing—original draft, and writing—review & editing. VP: conceptualization, data curation, investigation, and resources. PN: data curation, investigation, and resources. XD: data curation, formal analysis, and software. LS: investigation. YJT: conceptualization and writing—review & editing. HT: conceptualization. YY: conceptualization. GIB: conceptualization. G-FZ: conceptualization, data curation, investigation, resources, and writing—review & editing. CMK: conceptualization, methodology, resources, supervision, and writing—review & editing. BA:

conceptualization, formal analysis, funding acquisition, project administration, supervision, and writing—review & editing.

Author Contributions

Hongyuan Zhang: Conceptualization; data curation; formal analysis; investigation; methodology; project administration; resources; validation; visualization; writing – original draft; writing – review and editing. **Vijitha Puviindran:** Conceptualization; data curation; investigation; resources. **Puviindran Nadesan:** Data curation; investigation; resources. **Xiruo Ding:** Data curation; formal analysis; software. **Leyao Shen:** Investigation. **Yuning J Tang:** Conceptualization; writing – review and editing. **Hidetoshi Tsushima:** Conceptualization. **Yasuhito Yahara:** Conceptualization. **Ga I Ban:** Conceptualization. **Guo-Fang Zhang:** Conceptualization; data curation; investigation; resources; writing – review and editing. **Courtney M Karner:** Conceptualization; methodology; resources; supervision; writing – review and editing. **Benjamin A. Alman:** Conceptualization; funding acquisition; project administration; supervision; writing – review and editing.

Peer Review

The peer review history for this article is available at <https://publons.com/publon/10.1002/jbmr.4532>.

Data Availability Statement

The data that support the findings of this study are available from the corresponding author upon reasonable request.

References

1. Walden MJ, Murphey MD, Vidal JA. Incidental enchondromas of the knee. *Am J Roentgenol*. 2008;190(6):1611-1615.
2. Hong ED, Carrino JA, Weber KL, Fayad LM. Prevalence of shoulder enchondromas on routine MR imaging. *Clin Imaging*. 2011;35(5):378-384.
3. Bovée JVMG, Hogendoorn PCW, Wunder JS, Alman BA. Cartilage tumours and bone development: molecular pathology and possible therapeutic targets. *Nat Rev Cancer*. 2010;10(7):481-488.
4. Qasem SA, DeYoung BR. Cartilage-forming tumors. *Semin Diagn Pathol*. 2014;31(1):10-20.
5. Angelini A, Guerra G, Mavrogenis AF, Pala E, Picci P, Ruggieri P. Clinical outcome of central conventional chondrosarcoma. *J Surg Oncol*. 2012;106(8):929-937.
6. Amary MF, Damato S, Halai D, et al. Ollier disease and Maffucci syndrome are caused by somatic mosaic mutations of IDH1 and IDH2. *Nat Genet*. 2011;43(12):1262-1265.
7. Amary MF, Bacsi K, Maggiani F, et al. IDH1 and IDH2 mutations are frequent events in central chondrosarcoma and central and periosteal chondromas but not in other mesenchymal tumours. *J Pathol*. 2011;224(3):334-343.
8. Pansuriya TC, van Eijk R, d'Adamo P, et al. Somatic mosaic IDH1 and IDH2 mutations are associated with enchondroma and spindle cell hemangioma in Ollier disease and Maffucci syndrome. *Nat Genet*. 2011;43(12):1256-1261.
9. Meijer D, de Jong D, Pansuriya TC, et al. Genetic characterization of mesenchymal, clear cell, and dedifferentiated chondrosarcoma. *Genes Chromosomes Cancer*. 2012;51(10):899-909.
10. Zhang H, Alman BA. Enchondromatosis and growth plate development. *Curr Osteoporos Rep*. 2021;19(1):40-49.

11. Dang L, White DW, Gross S, et al. Cancer-associated IDH1 mutations produce 2-hydroxyglutarate. *Nature*. 2009;462(7274):739-744.
12. Zhao S, Lin Y, Xu W, et al. Glioma-derived mutations in IDH1 dominantly inhibit IDH1 catalytic activity and induce HIF-1 α . *Science (New York, NY)*. 2009;324(5924):261-265.
13. Leonardi R, Subramanian C, Jackowski S, Rock CO. Cancer-associated isocitrate dehydrogenase mutations inactivate NADPH-dependent reductive carboxylation. *J Biol Chem*. 2012;287(18):14615-14620.
14. Yang M, Soga T, Pollard PJ. Oncometabolites: linking altered metabolism with cancer. *J Clin Invest*. 2013;123(9):3652-3658.
15. Chowdhury R, Yeoh KK, Tian YM, et al. The oncometabolite 2-hydroxyglutarate inhibits histone lysine demethylases. *EMBO Rep*. 2011;12(5):463-469.
16. Xu W, Yang H, Liu Y, et al. Oncometabolite 2-hydroxyglutarate is a competitive inhibitor of α -ketoglutarate-dependent dioxygenases. *Cancer Cell*. 2011;19(1):17-30.
17. Lu C, Ward PS, Kapoor GS, et al. IDH mutation impairs histone demethylation and results in a block to cell differentiation. *Nature*. 2012;483(7390):474-478.
18. Turcan S, Rohle D, Goenka A, et al. IDH1 mutation is sufficient to establish the glioma hypermethylator phenotype. *Nature*. 2012;483(7390):479-483.
19. Figueroa ME, Abdel-Wahab O, Lu C, et al. Leukemic IDH1 and IDH2 mutations result in a hypermethylation phenotype, disrupt TET2 function, and impair hematopoietic differentiation. *Cancer Cell*. 2010;18(6):553-567.
20. Jin Y, Elalaf H, Watanabe M, et al. Mutant IDH1 dysregulates the differentiation of mesenchymal stem cells in association with gene-specific histone modifications to cartilage- and bone-related genes. *PLoS One*. 2015;10(7):e0131998.
21. Suijker J, Oosting J, Koornneef A, et al. Inhibition of mutant IDH1 decreases D-2-HG levels without affecting tumorigenic properties of chondrosarcoma cell lines. *Oncotarget*. 2015;6(14):12505-12519.
22. Cojocaru E, Wilding C, Engelman B, Huang P, Jones RL. Is the IDH1 mutation a good target for chondrosarcoma treatment? *Curr Mol Biol Rep*. 2020;6(12):1-9.
23. Pathmanapan S, Ilkayeva O, Martin JT, et al. Mutant IDH and non-mutant chondrosarcomas display distinct cellular metabolomes. *Cancer Metab*. 2021;9(1):13.
24. Wise DR, Thompson CB. Glutamine addiction: a new therapeutic target in cancer. *Trends Biochem Sci*. 2010;35(8):427-433.
25. Altman BJ, Stine ZE, Dang CV. From Krebs to clinic: glutamine metabolism to cancer therapy. *Nat Rev Cancer*. 2016;16(10):619-634.
26. Yu Y, Newman H, Shen L, et al. Glutamine metabolism regulates proliferation and lineage allocation in skeletal stem cells. *Cell Metab*. 2019;29(4):966-978.e4.
27. Stegen S, Rinaldi G, Loopmans S, et al. Glutamine metabolism controls chondrocyte identity and function. *Dev Cell*. 2020;53(5):530-44.e8.
28. Crawford J, Cohen HJ. The essential role of L-glutamine in lymphocyte differentiation in vitro. *J Cell Physiol*. 1985;124(2):275-282.
29. Johnson MO, Wolf MM, Madden MZ, et al. Distinct regulation of Th17 and Th1 cell differentiation by glutaminase-dependent metabolism. *Cell*. 2018;175(7):1780-95.e19.
30. Wang Y, Huang Y, Zhao L, Li Y, Zheng J. Glutaminase 1 is essential for the differentiation, proliferation, and survival of human neural progenitor cells. *Stem Cells Dev*. 2014;23(22):2782-2790.
31. Izquierdo-Garcia JL, Viswanath P, Eriksson P, et al. IDH1 mutation induces reprogramming of pyruvate metabolism. *Cancer Res*. 2015;75(15):2999-3009.
32. Salamanca-Cardona L, Shah H, Poot AJ, et al. In vivo imaging of glutamine metabolism to the oncometabolite 2-hydroxyglutarate in IDH1/2 mutant tumors. *Cell Metab*. 2017;26(6):830-41.e3.
33. Seltzer MJ, Bennett BD, Joshi AD, et al. Inhibition of glutaminase preferentially slows growth of glioma cells with mutant IDH1. *Cancer Res*. 2010;70(22):8981-8987.
34. Matre P, Velez J, Jacamo R, et al. Inhibiting glutaminase in acute myeloid leukemia: metabolic dependency of selected AML subtypes. *Oncotarget*. 2016;7(48):79722-79735.

35. Peterse EFP, Niessen B, Addie RD, et al. Targeting glutaminolysis in chondrosarcoma in context of the IDH1/2 mutation. *Br J Cancer*. 2018;118(8):1074-1083.
36. Emadi A, Jun SA, Tsukamoto T, Fathi AT, Minden MD, Dang CV. Inhibition of glutaminase selectively suppresses the growth of primary acute myeloid leukemia cells with IDH mutations. *Exp Hematol*. 2014;42(4):247-251.
37. Stegen S, Devignes C-S, Torrekens S, Van Looveren R, Carmeliet P, Carmeliet G. Glutamine metabolism in osteoprogenitors is required for bone mass accrual and PTH-induced bone anabolism in male mice. *J Bone Miner Res*. 2021;36(3):604-616.
38. Sharma D, Yu Y, Shen L, Zhang G-F, Karner CM. SLC1A5 provides glutamine and asparagine necessary for bone development in mice. *eLife*. 2021;10:e71595.
39. Hirata M, Sasaki M, Cairns RA, et al. Mutant IDH is sufficient to initiate enchondromatosis in mice. *Proc Natl Acad Sci*. 2015;112(9):2829-2834.
40. Mingote S, Masson J, Gellman C, et al. Genetic pharmacotherapy as an early CNS drug development strategy: testing glutaminase inhibition for schizophrenia treatment in adult mice. *Front Syst Neurosci*. 2015;9:165.
41. Long F, Zhang XM, Karp S, Yang Y, McMahon AP. Genetic manipulation of hedgehog signaling in the endochondral skeleton reveals a direct role in the regulation of chondrocyte proliferation. *Development*. 2001;128(24):5099-5108.
42. Chen M, Lichtler AC, Sheu TJ, et al. Generation of a transgenic mouse model with chondrocyte-specific and tamoxifen-inducible expression of Cre recombinase. *Genesis*. 2007;45(1):44-50.
43. Shultz LD, Lyons BL, Burzenski LM, et al. Human lymphoid and myeloid cell development in NOD/LtSz-scid IL2R gamma null mice engrafted with mobilized human hemopoietic stem cells. *J Immunol*. 2005;174(10):6477-6489.
44. Zhang H, Wei Q, Tsushima H, et al. Intracellular cholesterol biosynthesis in enchondroma and chondrosarcoma. *JCI Insight*. 2019;5:e127232.
45. Nicolle R, Ayadi M, Gomez-Brouchet A, et al. Integrated molecular characterization of chondrosarcoma reveals critical determinants of disease progression. *Nat Commun*. 2019;10(1):4622.
46. Liao Y, Long JT, Gallo CJR, Mirando AJ, Hilton MJ. Isolation and culture of murine primary chondrocytes: costal and growth plate cartilage. In Hilton MJ, ed. *Skeletal development and repair: methods and protocols*. New York, NY: Springer US; 2021 pp 415-423.
47. Robinson MM, Mcbryant SJ, Tsukamoto T, et al. Novel mechanism of inhibition of rat kidney-type glutaminase by bis-2-(5-phenylacetamido-1,2,4-thiadiazol-2-yl)ethyl sulfide (BPTES). *Biochem J*. 2007;406(3):407-414.
48. Campbell VT, Nadesan P, Ali SA, et al. Hedgehog pathway inhibition in chondrosarcoma using the smoothed inhibitor IPI-926 directly inhibits sarcoma cell growth. *Mol Cancer Ther*. 2014;13(5):1259-1269.
49. Carey BW, Finley LWS, Cross JR, Allis CD, Thompson CB. Intracellular α -ketoglutarate maintains the pluripotency of embryonic stem cells. *Nature*. 2015;518(7539):413-416.
50. Hwang I-Y, Kwak S, Lee S, et al. Psat1-dependent fluctuations in α -ketoglutarate affect the timing of ESC differentiation. *Cell Metab*. 2016;24(3):494-501.
51. Sullivan LB, Gui DY, Hosios AM, Bush LN, Freinkman E, Vander Heiden MG. Supporting aspartate biosynthesis is an essential function of respiration in proliferating cells. *Cell*. 2015;162(3):552-563.
52. Birsoy K, Wang T, Chen WW, Freinkman E, Abu-Remaileh M, Sabatini DM. An essential role of the mitochondrial electron transport chain in cell proliferation is to enable aspartate synthesis. *Cell*. 2015;162(3):540-551.
53. Qing G, Li B, Vu A, et al. ATF4 regulates MYC-mediated neuroblastoma cell death upon glutamine deprivation. *Cancer Cell*. 2012;22(5):631-644.
54. Ye J, Kumanova M, Hart LS, et al. The GCN2-ATF4 pathway is critical for tumour cell survival and proliferation in response to nutrient deprivation. *EMBO J*. 2010;29(12):2082-2096.
55. Zhang J, Fan J, Venneti S, et al. Asparagine plays a critical role in regulating cellular adaptation to glutamine depletion. *Mol Cell*. 2014;56(2):205-218.
56. Alkan HF, Walter KE, Luengo A, et al. Cytosolic aspartate availability determines cell survival when glutamine is limiting. *Cell Metab*. 2018;28(5):706-20.e6.